Chapter 6

A Model for the Role of the Angiopoietins in Angiogenesis

In this chapter, we formulate a model of angiogenesis that includes the role of the angiopoietins, a recently discovered family of growth factors that have emerged as critical regulators of angiogenesis and, in particular, of the balance between vascular quiescence, regression and growth (see section 1.5.5). The model differs from those of chapters 4 and 5 in that it is of the continuum (macroscopic) type and deals with EC density, as opposed to individual EC. Nevertheless, the model is formulated using the reinforced random walk framework, so transition to an individual cell-based model would be mathematically straightforward.

There has been a large volume of research [1, 9, 158, 165] on the angiopoietins since their initial discovery [41, 99] and much is now known about their expression patterns and regulatory effects. However, the only mathematical modelling work to include the angiopoietins to date has been [8]. In contrast to [8], which consists of ODEs for spatially averaged quantities, the model developed in this chapter focusses on the spatial development of the capillary network itself and the mechanisms whereby Ang-1 and Ang-2 stabilise and destabilise vascular structures. This approach has the advantage of being able to capture spatially non-homogeneous behaviour, whilst formulating a discrete form of the model offers the possibility of capturing microscopic features of the emergent capillary network. The model is also used to suggest potential strategies for therapeutic manipulation of angiogenesis via the angiopoietins.

In section 6.1, the mathematical model is constructed. The numerical method used to solve the equations is described in section 6.2 and the model parameters are discussed in section 6.3. The results are presented in section 6.4 and discussed in section 6.5.

6.1 The Mathematical Model

We construct the model on the domain $(x, y) \in \Omega = [0, L] \times [0, l]$, $t \in [0, T]$. The tumour is positioned at $(x, y) = (L/2, l)$ and a nearby capillary is at $y = 0$. For angiogenesis to succeed, EC from this capillary must cross the ECM and reach the tumour.

The quantities we wish to model are EC density (p) and the concentrations of VEGF (v), which is the principal angiogenic stimulus, and the angiopoietins, Ang-1 (a_1) and Ang-2 (a_2).

6.1.1 Model Assumptions

The principal model assumptions are as follows.

1. The tumour secretes VEGF, which is a chemoattractant for EC, at a constant rate. The VEGF diffuses through the tissue, establishing a chemotactic gradient to which the EC can respond. Uptake of VEGF by EC is negligible in comparison to the large quantities of VEGF produced by the tumour.

2. Experimental observations indicate that Ang-2 is expressed at high levels in localised areas of vascular remodelling, and is absent from areas in which the vasculature is quiescent or undergoing maturation [99]. There is increasing evidence to suggest that Ang-2 is expressed specifically at the tips of growing capillaries [1, 63, 99]. The precise stimulus for Ang-2 expression by EC is unclear; one possibility is that Ang-2 is expressed in response to some hypoxia-inducible factor or tumour-derived growth factor [111]. It is possible that Ang-2 is expressed by immature EC, whereas EC that have undergone some degree of maturation no longer express Ang-2 [70]. We therefore divide the EC into two classes: immature (or activated) cells, which do produce Ang-2,

and mature (or inactive) cells, which do not.

3. EC proliferation is observed mainly at the capillary tips [1, 11, 148], so we assume that only the immature cells undergo proliferation.

4. The situation in the parent vessel is different, in that the normally quiescent EC revert to a plastic phenotype (possibly in response to hypoxia) and *do* subsequently express Ang-2 [13]. We therefore assume that a tumour-derived signal, such as hypoxia or a diffusible growth factor, stimulates the endothelium of the pre-existing vasculature to become activated. Thus, the EC of the parent vessel are already in the immature state at the start of the mathematical model. Some authors have reported that Ang-2 expression in the vasculature precedes VEGF expression by the tumour [177], whilst others have reported that the two events are almost simultaneous [54, 167]. Here we treat both cases.

5. VEGF is a strong maturation signal for EC, so we assume that the VEGF concentration must be above a certain threshold level for maturation to take place. Above this level, the rate of maturation is assumed to be constant.

6. Ang-1 is naturally present throughout the tissue at a constant background level, a_0 [99], and is expressed by peri-endothelial support cells. These cells are associated with the maturing part of the vessel and we therefore assume that Ang-1 production is proportional to the density of mature EC.

7. The angiopoietins act in a paracrine manner, so diffusion of Ang-1 and Ang-2 is neglected.

8. The angiopoietins influence EC movement in the following way: Ang-2 acts as a destabilising factor, loosening cell–cell and cell–matrix contacts and thus allowing greater EC motility; Ang-1 helps to maintain vessels in a quiescent state by reducing EC motility.

9. The angiopoietins also influence EC proliferation and death rates. Experimental evidence indicates that Ang-2 must be present at approximately eight times the concentration of Ang-1 to completely block the effects of the latter [99]. If the local concentration of Ang-2 is below this threshold value, the EC are in a state of quiescence and there is no cell proliferation or death. If Ang-2 is locally present at eight or more times the concentration of Ang-1, the EC emerge from quiescence and become dependent on the survival signal of VEGF [95]. High levels of VEGF stimulate the EC to enter the cell division cycle,

resulting in proliferation; an absence of VEGF, however, results in apoptosis [119].

We have made some major simplifications here. For example, cells cannot simply be classified as mature or immature: there will, in reality, be a large number of maturity states as the cell progressively undergoes small changes. Similarly, the assumed threshold behaviour is unlikely to be a simple on–off switch. A gradual increase above a certain threshold would probably be more realistic. Nevertheless, we believe that such simplifications are necessary, as a first step, in order to formulate a model that captures the fundamental behaviour, but is mathematically tractable. Refinements can always be made at a later stage and the simple model will help to highlight which assumptions need to be reviewed.

6.1.2 The Endothelial Cell Dynamics

We wish to derive a PDE for EC density and use a continuum limit form of the type derived in chapter 3. This will enable the corresponding reinforced random walk model to be formulated via the transition probability function. Specifically, we use a PDE of the form:

$$\frac{\partial p}{\partial t} = D_p \nabla . \left(D\left(w\right) \nabla p - p \nabla \left(\ln \tau \left(w\right) \right) \right), \tag{6.1}$$

where $D_p > 0$ is constant. This allows for the dependence of the diffusion coefficient, $D\left(w\right)$, on the control substances, w. The transition rates for the corresponding master equation may be calculated as described in section 3.4.2.

We hypothesise that the respective stabilising and destabilising effects of Ang-1 and Ang-2 act by altering the motility coefficient of the EC. Thus Ang-1 will help to stabilise vessels by decreasing the motility coefficient, keeping the EC in place, whereas Ang-2 will destabilise vessels by increasing the motility coefficient, allowing the EC to move more freely and respond to any chemotactic gradients they may detect. We therefore take

$$D\left(a_1, a_2\right) = \left(1 + s_1 a_1\right)^{-\alpha} \left(1 + s_2 a_2\right)^{\beta}, \tag{6.2}$$

where $D_p, s_1, s_2, \alpha, \beta \geq 0$ are constants.

Whilst (6.2) describes the dependence of the rate of EC movement on a_1 and a_2, the transition probability function, τ, will govern the directional preference of the

EC. VEGF and Ang-1 are known to be chemoattractants for EC, whilst Ang-2 is not thought to have any chemotactic effects [77, 172]. We therefore take $\tau(w) = \tau(v, a_1)$. By (3.40), we have

$$\ln \tau = \frac{1}{D_p}\left(\int \chi_v(v)\, dv + \int \chi_1(a_1)\, da_1\right),$$

where $\chi_v(v)$ and $\chi_1(a_1)$ are the chemotactic sensitivities to VEGF and Ang-1 respectively.

As in chapter 5, we choose the sensitivities to be:

$$\chi_v(v) = \gamma D_p \tfrac{s_4 - s_3}{(v+s_3)(v+s_4)}, \quad \chi_1(a_1) = \sigma D_p \tfrac{s_6 - s_5}{(a_1+s_5)(a_1+s_6)},$$

where $0 < s_3, s_5 < s_4, s_6$ and $\gamma, \sigma \geq 0$ are constants. The chemotactic flux is therefore directed up gradients of VEGF and Ang-1.

Hence the transition probability function is given by:

$$\tau(v, a_1) = \left(\frac{v + s_3}{v + s_4}\right)^{\gamma} \left(\frac{a_1 + s_5}{a_1 + s_6}\right)^{\sigma}. \tag{6.3}$$

We now divide the EC into two categories: immature and mature, with densities denoted by $p_1(x, y, t)$ and $p_2(x, y, t)$ respectively. Both populations follow the same rules for cell movement, so both the PDE for p_1 and the PDE for p_2 will contain a term of the form (6.1). In addition, there will be a transfer of cells from the first population to the second, representing the maturation process. We assume that, provided the VEGF is above some threshold level, $v_c \geq 0$, this transfer takes place at constant rate, $r \geq 0$. The PDE for immature cells should also include a proliferation/death term, Γ (discussed below). We therefore have the following pair of PDEs:

$$\frac{\partial p_1}{\partial t} = D_p \nabla . \left(D(a_1, a_2)\, \nabla p_1 - p_1 \frac{\nabla \tau}{\tau}\right) + \Gamma - rH(v - v_c)\, p_1, \tag{6.4}$$

$$\frac{\partial p_2}{\partial t} = D_p \nabla . \left(D(a_1, a_2)\, \nabla p_2 - p_2 \frac{\nabla \tau}{\tau}\right) + rH(v - v_c)\, p_1. \tag{6.5}$$

It would be possible to take different diffusion coefficients for the mature and immature EC populations. One would expect mature EC to be less motile and one could even argue for omitting the movement terms for the mature EC altogether (the effects of this will be discussed in section 6.4). However, we take the view that there is no *inherent* reduction in motility as the EC undergo maturation, rather it is the external chemical signals that determine motility, via the diffusivity function (6.2).

We model the VEGF–angiopoietin interplay shown in Figure 1.11 via the proliferation/death term, Γ, for the immature EC:

$$\Gamma = QH\left(a_2 - \lambda a_1\right) p_1 \left(1 - \frac{p_1\left(v + \theta_1\right)}{p_m\left(v + \theta_2\right)}\right), \tag{6.6}$$

where $Q, p_m, \lambda \geq 0$ and $\theta_1 > \theta_2 > 0$ are constants.

This function is modulated by the heaviside step function, so $\Gamma = 0$ if $\lambda a_1 > a_2$. Experimental evidence [99] indicates that Ang-2 must be present at approximately eight times the concentration of Ang-1 to completely block the effects of the latter. We therefore take $\lambda = 8$. Thus if Ang-1 locally outweighs Ang-2, the EC will be stabilised and no proliferation or death will occur, whereas if Ang-2 outweighs Ang-1, the proliferation/death function is switched on. In the latter case, Γ is a logistic growth term with a VEGF-dependent carrying capacity given by

$$C = \frac{p_m\left(v + \theta_2\right)}{v + \theta_1}. \tag{6.7}$$

If the VEGF concentration is high then the carrying capacity is high and vice versa. So at high VEGF concentrations, $\Gamma > 0$, indicating proliferation, whereas at low concentrations, $\Gamma < 0$, indicating cell death.

6.1.3 The Substrate Dynamics

In the interior of the domain (i.e. in the ECM), we consider the following kinetic interactions between the three substrates, VEGF, Ang-1 and Ang-2.

Ang-1 is uniformly present at a low level throughout the tissue [99], so we assume that Ang-1 will tend to evolve to some constant background level, $a_0 \geq 0$. We also include an Ang-1 production term associated with the mature EC population. This may be thought of as being derived from peri-endothelial support cells (such as pericytes) associated with mature vessels:

$$\frac{\partial a_1}{\partial t} = b_1 p_2 + \mu_1\left(a_0 - a_1\right), \tag{6.8}$$

where $b_1, \mu_1 \geq 0$ are constants.

Ang-2 is assumed to be expressed by immature EC at constant rate. Including a natural decay term gives:

$$\frac{\partial a_2}{\partial t} = b_2 p_1 - \mu_2 a_2, \tag{6.9}$$

where $b_2, \mu_2 \geq 0$ are constants.

We are assuming that uptake of VEGF by EC is negligible, so the only kinetic term for VEGF is natural decay. The addition of Fickian diffusion gives the following PDE:

$$\frac{\partial v}{\partial t} = D_v \nabla^2 v - \mu_v v, \tag{6.10}$$

where $D_v, \mu_v \geq 0$ are constants.

6.1.4 Initial and Boundary Conditions

The secretion of VEGF by the tumour is included by prescribing a flux of VEGF into the ECM from the tumour. There is no flux of EC at this boundary, so we have the following boundary conditions at $y = l$:

$$D_v \frac{\partial v}{\partial y} = J_v(x), \tag{6.11}$$

$$D(a_1, a_2) \frac{\partial p_i}{\partial y} - p_i \frac{\partial}{\partial y} \ln \tau = 0 \quad (i = 1, 2). \tag{6.12}$$

Similarly, we impose no-flux boundary conditions for all the quantities on the other three boundaries of the ECM ($y = 0$, $x = 0$ and $x = L$).

For the source function, J_v, we take a unimodal function of the same form (5.36) as in chapter 5:

$$J_v(x) = \frac{v_0 \sigma_0}{L} \left(1 - \cos \frac{2\pi x}{L}\right)^{m_0}, \tag{6.13}$$

where $\sigma_0 = \left(\int_0^1 (1 - \cos 2\pi x)^{m_0} \, dx\right)^{-1}$ and $v_0, m_0 \geq 0$ are constants. In the case where Ang-2 expression by the EC precedes VEGF expression by the tumour, we simply delay the source term by setting $J_v = 0$ for $0 \leq t < T_d$.

Initially, there is no VEGF or Ang-2 in the system and Ang-1 is uniformly present at its background level. EC are present only at the parent capillary at $y = 0$ and are assumed to have reverted to the immature state. We model this latter condition by taking p_1 to be linearly decreasing in the bottom tenth of the ECM nearest to the parent capillary. The initial conditions thus take the form

$$v(x, y, 0) = 0, \tag{6.14}$$

$$a_1(x, y, 0) = a_0, \tag{6.15}$$

$$
\begin{aligned}
a_2(x,y,0) &= 0, && (6.16)\\
p_1(x,y,0) &= \left\{ \begin{array}{ll} p_0\left(1-\frac{10y}{l}\right), & 0 \le y \le \frac{l}{10} \\ 0, & \frac{l}{10} \le y \le l \end{array} \right\}, && (6.17)\\
p_2(x,y,0) &= 0, && (6.18)
\end{aligned}
$$

where $p_0 > 0$ is a constant.

6.1.5 Non-Dimensionalisation

Let

$$v' = \frac{v}{a_0}, \quad a_1' = \frac{a_1}{a_0}, \quad a_2' = \frac{a_2}{a_0}, \quad p_1' = \frac{p_1}{p_0}, \quad p_2' = \frac{p_2}{p_0}, \quad t' = \frac{D_p}{L^2}t, \quad x' = \frac{x}{L}, \quad y' = \frac{y}{L}.$$

The constants resulting from this scaling are rewritten in the following as K_i (see Table 6.1).

The system (6.2)–(6.10) becomes (dropping the dashes):

$$
\begin{aligned}
\frac{\partial p_1}{\partial t} &= \nabla.\left(D(a_1,a_2)\nabla p_1 - p_1\frac{\nabla\tau}{\tau}\right) + K_1 H(a_2-\lambda a_1)\, p_1\left(1-K_2 p_1\frac{v+K_3}{v+K_4}\right)\\
&\quad -K_5 H(v-K_6)\, p_1, && (6.19)\\
\frac{\partial p_2}{\partial t} &= \nabla.\left(D(a_1,a_2)\nabla p_2 - p_2\frac{\nabla\tau}{\tau}\right) + K_5 H(v-K_6)\, p_1, && (6.20)\\
\frac{\partial v}{\partial t} &= K_7\nabla^2 v - K_8 v, && (6.21)\\
\frac{\partial a_1}{\partial t} &= K_9 p_2 + K_{10}(1-a_1), && (6.22)\\
\frac{\partial a_2}{\partial t} &= K_{11} p_1 - K_{12} a_2, && (6.23)
\end{aligned}
$$

on $(x,y) \in \Omega = [0,1] \times \left[0, \frac{l}{L}\right]$, $t \in \left[0, \frac{TD_p}{L^2}\right]$, where

$$
\begin{aligned}
D(a_1,a_2) &= (1+K_{13}a_1)^{-\alpha}(1+K_{14}a_2)^{\beta}, && (6.24)\\
\tau(v,a_1) &= \left(\frac{v+K_{15}}{v+K_{16}}\right)^{\gamma}\left(\frac{a_1+K_{17}}{a_1+K_{18}}\right)^{\sigma}. && (6.25)
\end{aligned}
$$

The boundary conditions at the tumour side of the ECM (6.11), (6.12) become

$$
\begin{aligned}
\frac{\partial v}{\partial y} &= K_{19}\left(1-\cos(2\pi x)\right)^{m_0}, \text{ on } y = \frac{l}{L}, && (6.26)\\
D(a_1,a_2)\frac{\partial p_i}{\partial y} - p_i\frac{\partial}{\partial y}\ln\tau &= 0, \text{ on } y = \frac{l}{L}\ (i=1,2). && (6.27)
\end{aligned}
$$

i	K_i	i	K_i	i	K_i	i	K_i
1	$\frac{QL^2}{D_p}$	2	$\frac{p_0}{p_m}$	3	$\frac{\theta_1}{a_0}$	4	$\frac{\theta_2}{a_0}$
5	$\frac{rL^2}{D_p}$	6	$\frac{v_c}{a_0}$	7	$\frac{D_v}{D_p}$	8	$\frac{L^2\mu_v}{D_p}$
9	$\frac{b_1 p_0 L^2}{a_0 D_p}$	10	$\frac{L^2\mu_1}{D_p}$	11	$\frac{b_2 p_0 L^2}{a_0 D_p}$	12	$\frac{L^2\mu_2}{D_p}$
13	$a_0 s_1$	14	$a_0 s_2$	15	$\frac{s_3}{a_0}$	16	$\frac{s_4}{a_0}$
17	$\frac{s_5}{a_0}$	18	$\frac{s_6}{a_0}$	19	$\frac{v_0\sigma_0}{a_0 D_v}$		

Table 6.1: Constants resulting from the non-dimensionalisation of the model.

The remaining no-flux boundary conditions are

$$\frac{\partial v}{\partial y} = 0, \text{ on } y = 0, \tag{6.28}$$

$$D(a_1, a_2)\frac{\partial p_i}{\partial y} - p_i \frac{\partial}{\partial y}\ln\tau = 0, \text{ on } y = 0 \ (i = 1, 2), \tag{6.29}$$

$$\frac{\partial v}{\partial x} = 0, \text{ on } x = 0, 1, \tag{6.30}$$

$$D(a_1, a_2)\frac{\partial p_i}{\partial x} - p_i \frac{\partial}{\partial x}\ln\tau = 0, \text{ on } x = 0, 1 \ (i = 1, 2). \tag{6.31}$$

Finally, the initial conditions (6.14)–(6.18) become

$$v(x, y, 0) = 0, \tag{6.32}$$

$$a_1(x, y, 0) = 1, \tag{6.33}$$

$$a_2(x, y, 0) = 0, \tag{6.34}$$

$$p_1(x, y, 0) = \left\{ \begin{array}{ll} 1 - 10\frac{L}{l}y, & 0 \le y \le \frac{l}{10L}, \\ 0, & \frac{l}{10L} \le y \le \frac{l}{L} \end{array} \right\}, \tag{6.35}$$

$$p_2(x, y, 0) = 0. \tag{6.36}$$

Note that the PDE for VEGF (6.21) is decoupled from the rest of the system and, subject to the initial and boundary conditions (6.26), (6.28), (6.30), (6.32), may be solved independently. The solution rapidly approaches its steady state value, which, for $m_0 \in \mathbb{Z}$, is given by

$$v_s(x, y) = 2K_{19}\sum_{n=0}^{m_0} A_n \cos(2n\pi x)\cosh\left(\sqrt{\frac{K_8}{K_7} + 4n^2\pi^2}\, y\right), \tag{6.37}$$

where the A_n are Fourier coefficients.

Length scale	$l = L = 0.05$ mm
Reference EC density	$p_0 = 10^{-5}$ μM
Maximum EC density	$p_m = 10^{-4}$ μM
Background Ang-1 density	$a_0 = 10^{-3}$ μM
Angiopoietin decay rates	$\mu_1 = \mu_2 = 4.56$ h^{-1}
Ang-1 production rate	$b_1 = 2280$ h^{-1}
Ang-2 production rate	$b_2 = 18240$ h^{-1}
VEGF decay rate	$\mu_v = 0.456$ h^{-1}
EC diffusion coefficient	$D_p = 3.6 \times 10^{-6}$ mm^{2}h^{-1}
VEGF diffusion coefficient	$D_v = 3.6 \times 10^{-4}$ mm^{2}h^{-1}
VEGF production rate	$v_0 = 2 \times 10^{-6}$ μM mm^{2}h^{-1}
EC proliferation rate	$Q = 1.35$ h^{-1}
EC maturation rate	$r = 0.2$ h^{-1}
Threshold VEGF level	$v_c = 5 \times 10^{-4}$ μM
Diffusion sensitivity coefficients	$s_1 = s_2 = 10^3$ μM^{-1}
Chemotactic sensitivity coefficients	$s_3 = s_5 = 10^{-4}$ μM^{-1}
	$s_4 = s_6 = 10^{-2}$ μM^{-1}
Exponents	$\alpha = \beta = 1$
	$\gamma = 4$, $\sigma = 0$, $m_0 = 12$
Carrying capacity coefficients	$\theta_1 = 10^{-3}$ μM
	$\theta_2 = 10^{-5}$ μM

Table 6.2: Parameter values used in the numerical solutions.

6.2 The Method of Simulation

The system (6.19)–(6.36) is solved numerically. The reaction–diffusion PDEs (6.19)–(6.21) are solved using the Crank–Nicolson method described in appendix A. The ODEs (6.22), (6.23) are solved using the Euler method.

6.3 Parameter Values

The parameter values used in the numerical solutions are shown in Table 6.2. Where possible, these were taken from the biological literature, but the paucity of relevant experimental data means that the values of some of the parameters are unknown and had to be estimated.

EC densities. The initial EC density, $p_0 = 10^{-5}$ μM is based on an approximate EC length of 10 μm–100 μm, a width of 10 μm and a thickness of 1 μm [87]. The maximum density, $p_m = 10^{-4}$ μM, is an assumption that the EC density can increase

by a factor of no more than 10 above the base level (though in fact the carrying capacity (6.7) is generally less than this because of the VEGF dependence).

Background Ang-1 concentration. In [58], Ang-1 concentrations in the range 50 ng/ml – 300 ng/ml were used. For the background level, we use the lower end of this range which, taking the molecular weight of Ang-1 as 70 kDa [41, 71], is equivalent to approximately 10^{-3} μM.

Decay rates. For the angiopoietin decay rates, we use the enzyme decay rate quoted by [87] of $\mu = 4.56$ h^{-1}. We use the lower value of $\mu_v = 0.456$ h^{-1} for the VEGF decay rate so that the VEGF diffuses at a significant concentration throughout the ECM.

Diffusion coefficients. For the diffusion coefficients, we use the values of [87], $D_p = 3.6 \times 10^{-6}$ mm^{2}h^{-1}, $D_v = 3.6 \times 10^{-4}$ mm^{2}h^{-1}.

VEGF production rate. VEGF concentrations in the range 1 ng/ml – 200 ng/ml were used in [166]. Taking the molecular weight of VEGF as 40 kDa [55, 118], we choose the VEGF production rate, $v_0 = 2 \times 10^{-6}$ μM mm^{2}h^{-1}, so that the typical VEGF concentrations encountered by EC fall within this range.

EC proliferation rate. Although quiescent EC have a very low turnover rate, activated EC can, during angiogenesis, achieve high proliferation rates. For this reason, we take $Q = 1.35$ h^{-1}, which corresponds to a *minimum* doubling time of approximately one hour (although the doubling time is generally somewhat longer than this and is, in any case, constrained by the carrying capacity).

The remaining parameters in Table 6.2 are difficult to specify with any certainty. Simulations have been run over a range of values of these parameters to check robustness of the model (i.e. that small changes in the parameter values do not cause large changes in model predictions). For example, Figure 6.1 shows how the vascularisation time (defined as the time at which the EC density at $y = 1$ rises above 0.1) varies with respect to the exponents, α and β, in the EC motility coefficient (6.24). Unsurprisingly, the greater the inhibitory effect of Ang-1 on EC motility (the greater α), the longer the time taken for vascularisation; the greater the permissive effect of Ang-2 on EC motility (the greater β), the shorter the time taken for vascularisation. The values given in Table 6.2 were chosen to give reasonable, physiological results with respect to quantities such as travel times and angiopoietin

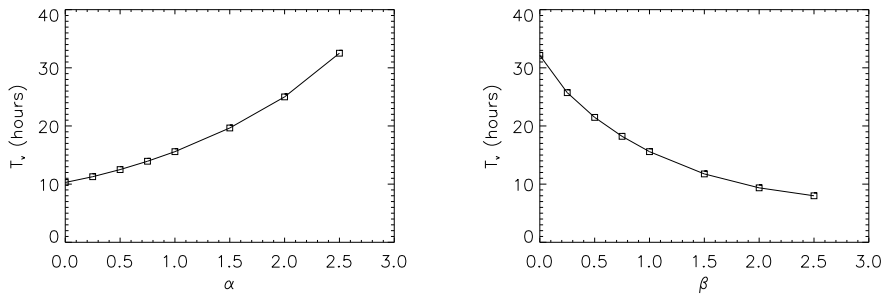

(a) (b)

Figure 6.1: Graphs of the vascularisation time, T_v, against the parameters: (a) α. (b) β.

concentrations.

Although EC have been observed to migrate up an Ang-1 concentration gradient [172], it is likely that VEGF is a much more powerful chemoattractant. For this reason, the simulations were run with $\sigma = 0$ in equation (6.25), i.e. with no chemotactic response to Ang-1. Setting $\sigma > 0$ slows angiogenesis because Ang-1 is generally higher towards the parent vessel and the Ang-1 gradient, in contrast to the VEGF gradient, therefore provides a chemotactic stimulus *away* from the tumour.

6.4 Results

Figures 6.2, 6.3, 6.4 and 6.5 respectively show time courses for the density of immature and mature EC and the concentrations of Ang-1 and Ang-2. Recall that the tumour is situated at $x = 0.5$, $y = 1.0$ and the parent vessel is located on the x-axis ($y = 0$). Ang-2 expression by the EC and VEGF expression by the tumour begin simultaneously at $t = 0$. The VEGF profile quickly reaches a diffusive steady state (see equation (6.37) and Figure 6.6), thus establishing a chemotactic gradient, which stimulates the EC to move towards the tumour.

The immature cells appear to move as a wave across the ECM and eventually reach the tumour (after 15.6 h), providing it with the blood supply it requires for sustained growth. Cells behind this wave mature to form a contiguous mass of mature cells between the leading edge of the neovasculature and the parent vessel. Immature

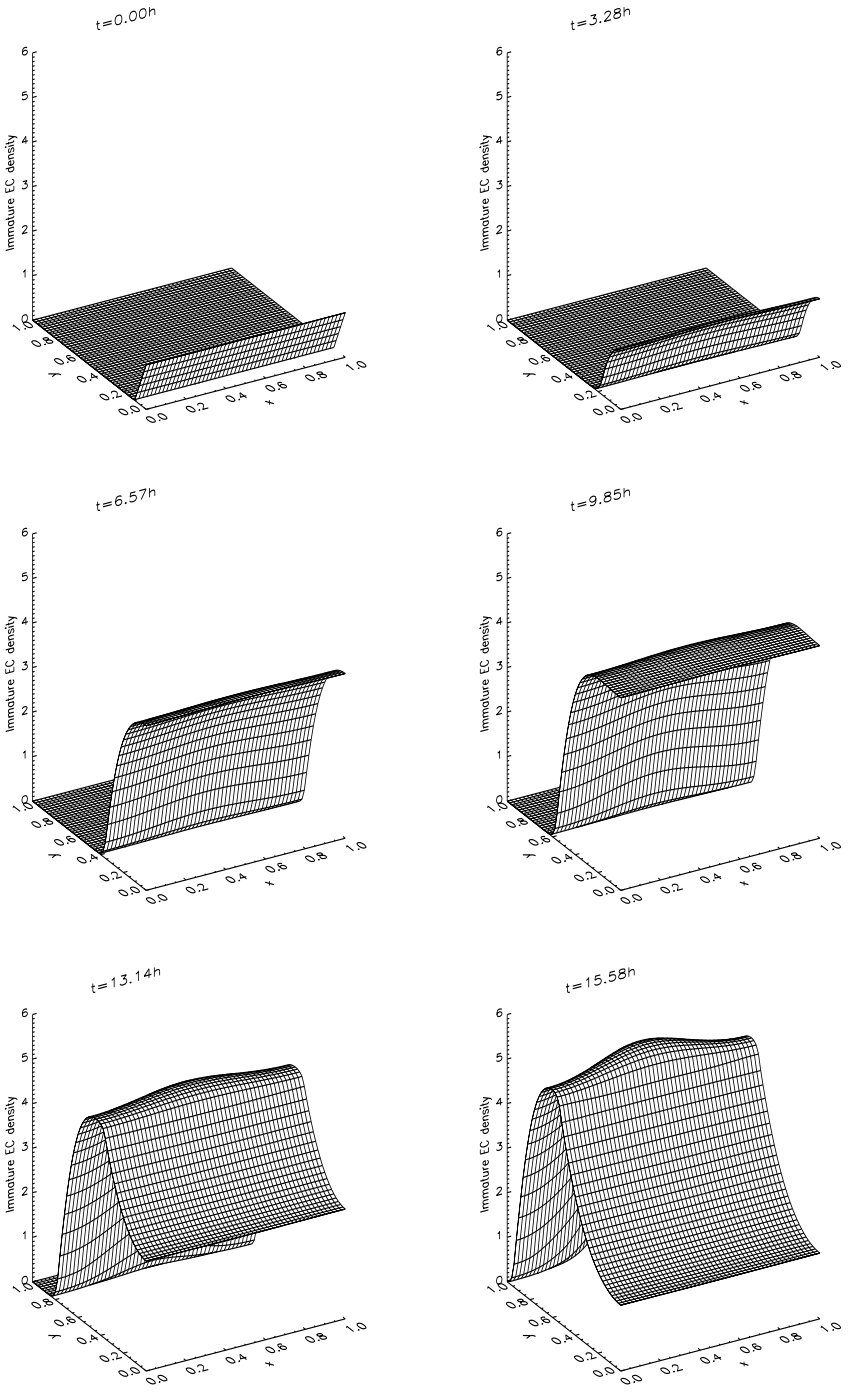

Figure 6.2: Time course for immature EC density.

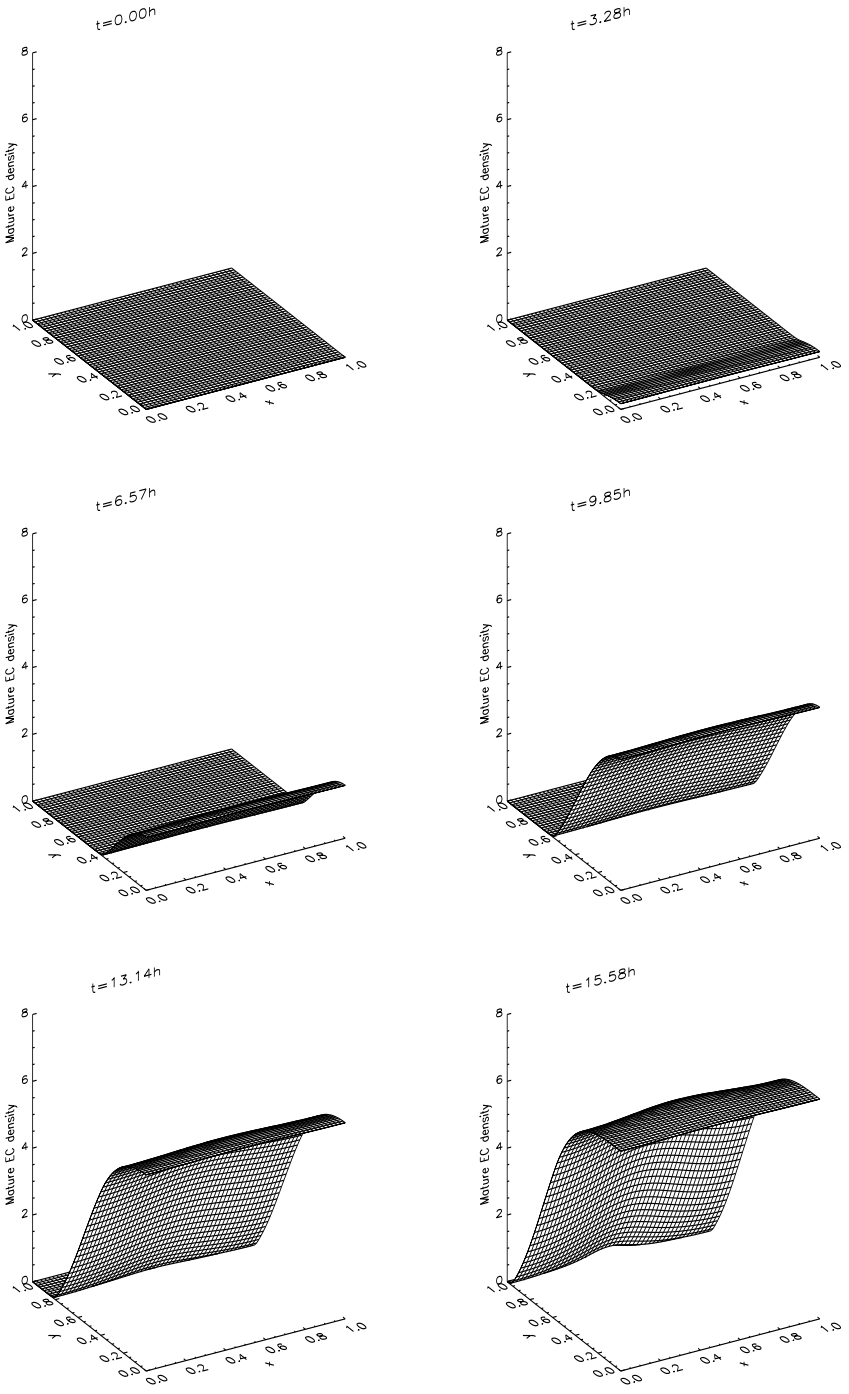

Figure 6.3: Time course for mature EC density.

cell density is at a maximum at the leading edge of the nascent capillary network (a region that shall be referred to as the capillary tips), whereas the mature cells are generally located behind the leading edge. Thus, consistent with experimental evidence [11, 148], the bulk of the angiogenic activity of migration and proliferation occurs at the tips of the nascent capillaries, with vessel maturation taking place between the tips and the parent vessel.

Unsurprisingly, Ang-2, expressed by immature cells, is at its highest level at the tips (Figure 6.5), whereas Ang-1 is expressed in the maturing part of the vessels (Figure 6.4). The angiogenic switch, regulated by Ang-1 and Ang-2 via (6.6), is therefore 'on' at the capillary tips, allowing cell proliferation/death and increasing motility, but 'off' nearer to the parent vessel, allowing stabilisation of the new vessels.

Figures 6.7 and 6.8 show cell density profiles in a simulation with no Ang-2 ($b_2 = 0$ in equation (6.9)). The proliferation function (6.6) is always 'off' because $a_2 \equiv 0$. There is therefore no mechanism for the replacement of immature cells, which have almost disappeared by the end of the simulation. In addition to the lack of EC proliferation, there is a substantial reduction in EC migration, largely due to the reduced EC motility. The EC do not reach the tumour and vascularisation fails to take place. This is consistent with observations [49] that Ang-2-deficient mice exhibit severe defects in postnatal vascular remodelling, indicating that Ang-2 is required for angiogenic outgrowth.

Figures 6.9 and 6.10 show cell density profiles in a simulation with no Ang-1 expression ($b_1 = 0$ in equation (6.8)). As in the full simulation, a wave of immature cells crosses the ECM, though this time more rapidly (reaching the tumour after just 12.7 h, as opposed to 15.6 h). The other major difference is that the density of immature cells does not peak at the leading edge of the neovasculature, as it does in Figure 6.2. Instead, immature cells are evenly distributed between the capillary tips and the parent vessel; this is because Ang-2 remains above threshold, so the proliferation/death function remains 'on', even away from the capillary tips. We believe that the continued presence of immature EC in vascularised areas is indicative of disrupted vessel stabilisation. This is in agreement with evidence [158] that, whilst Ang-1 is not required for the formation of the primary vasculature by embryonic vasculogenesis, it is necessary for subsequent vascular remodelling and vessel maturation. For example, knockout of the genes encoding Ang-1 results in a poorly organised vasculature with hyperpermeable vessels, disrupted interactions

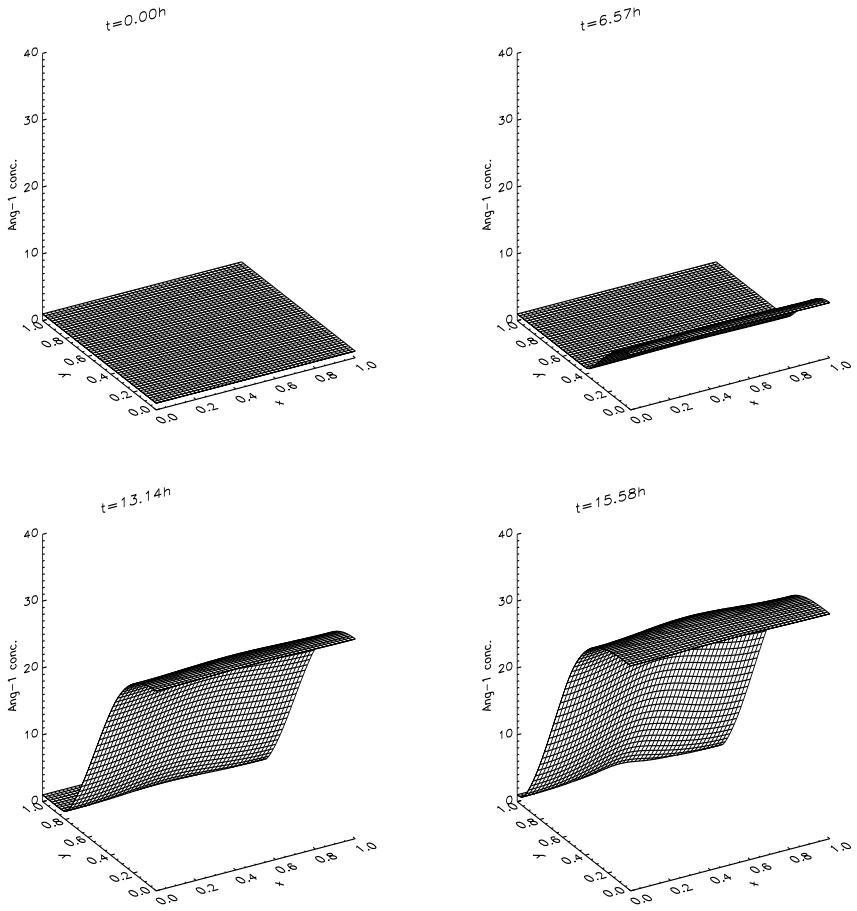

Figure 6.4: Time course for Ang-1 concentration.

between EC and their basement membrane and a lack of peri-endothelial support cells [13, 26, 162].

Figures 6.11 and 6.12 show cell density profiles in a simulation in which the Ang-2 production rate, b_2, is double the value shown in Table 6.2. The results are very similar to those with no Ang-1 expression (Figures 6.9 and 6.10), with the EC reaching the tumour in 11.5 h. Experimental data [96] indicate that over-expression of Ang-2 results in a phenotype very similar to knockout of Ang-1.

Conversely, doubling the Ang-1 production rate (Figures 6.13 and 6.14) reduces the angiogenic response in a similar fashion to removing Ang-2. The effects are not as severe, in that there is initially some EC proliferation and angiogenic outgrowth. This is because the immature cells are initially able to produce enough Ang-2 to block the Ang-1 signal and allow proliferation. However, Ang-1 soon regains control,

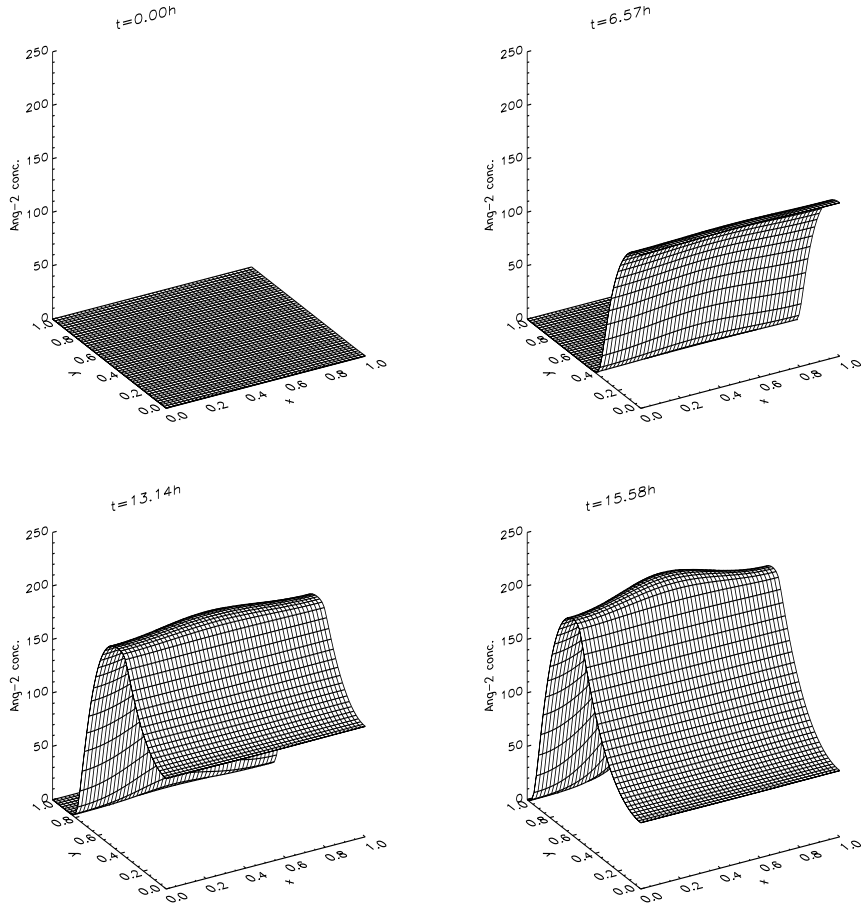

Figure 6.5: Time course for Ang-2 concentration.

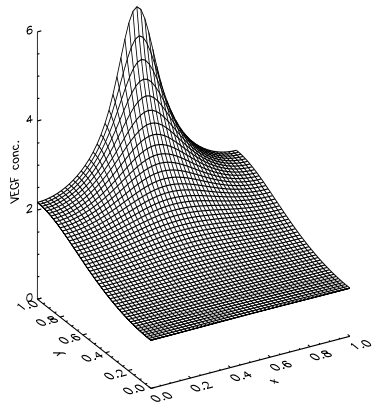

Figure 6.6: The steady state VEGF concentration.

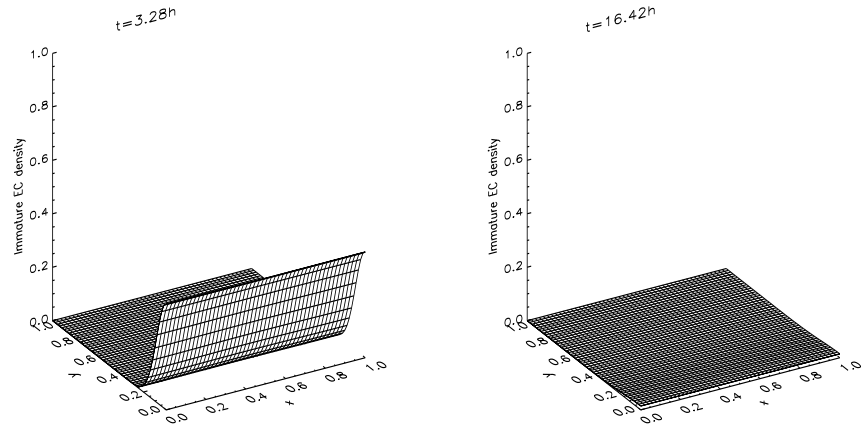

Figure 6.7: Time course for immature EC density with no Ang-2 ($b_2 = 0$).

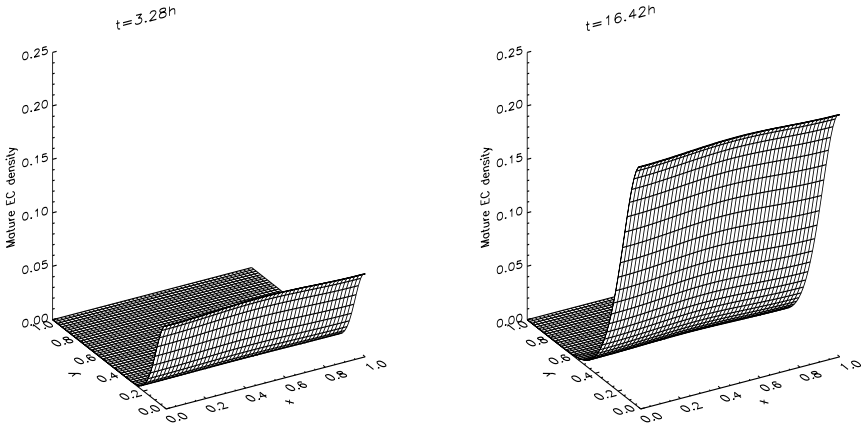

Figure 6.8: Time course for mature EC density with no Ang-2 ($b_2 = 0$).

the number of immature cells begin to fall and the angiogenic response slows almost to a halt.

Figure 6.15 shows the results of removing the VEGF source. Note that there is no cell maturation (because of the threshold level of VEGF required) and that the carrying capacity (6.7) is very low. Unsurprisingly, there is very little EC migration, and cell death reduces the population of immature cells to a low level. We interpret this result as vessel regression. This is consistent with evidence that Ang-2 effectively enables EC to enter a decision-making process. If a VEGF signal is detected, the EC will mount an angiogenic response by undergoing migration, proliferation and tubule formation; if no VEGF signal is detected, EC apoptosis will ensue [1]. Thus

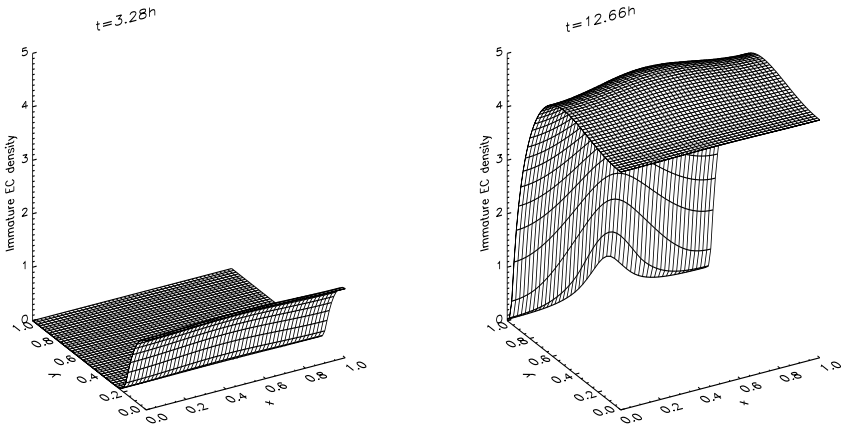

Figure 6.9: Time course for immature EC density with no Ang-1 expression ($b_1 = 0$).

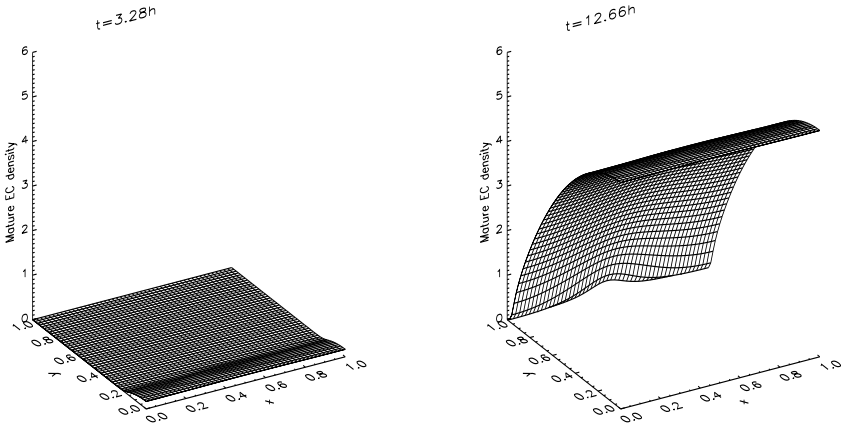

Figure 6.10: Time course for mature EC density with no Ang-1 expression ($b_1 = 0$).

co-expression of VEGF with Ang-2 leads to the formation of new vessels (as in Figure 6.2), but Ang-2 in the absence of VEGF (or any other mitogenic factor) results in vessel regression [95] (as in Figure 6.15).

In the case where Ang-2 expression by the EC precedes VEGF expression by the tumour by 1 h, vessel regression is also observed (results not shown). There is a period of time during which, as in Figure 6.15, the EC are exposed to Ang-2 but not to VEGF. Note that, in addition to the time before the source of VEGF is activated, there is a subsequent period, while VEGF diffuses throughout the ECM, for which the EC are deprived of any mitogenic stimulus. The process of regression begins and, even when VEGF expression is delayed by as little as one hour, cannot be

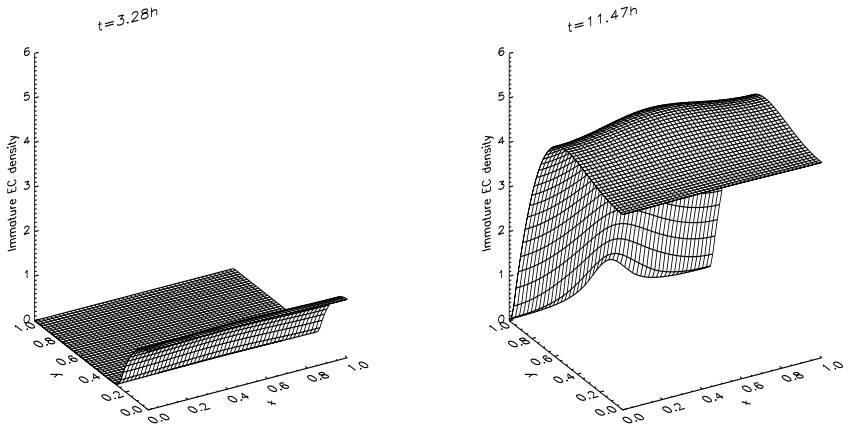

Figure 6.11: Time course for immature EC density with increased Ang-2 expression ($b_2 = 36480$ h^{-1}).

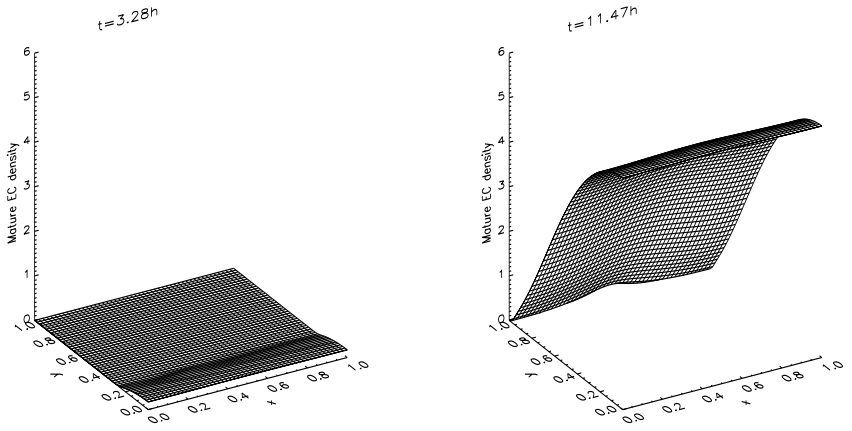

Figure 6.12: Time course for mature EC density with increased Ang-2 expression ($b_2 = 36480$ h^{-1}).

halted by the late arrival of the VEGF. This is because, by the time a VEGF signal is detected, EC density has fallen to such a level that the Ang-2 concentration is below the threshold required for proliferation. Hence, although there is no further cell death, neither is there any proliferation, no matter how much VEGF is detected, and the EC are consequently unable to mount an angiogenic response.

In the simulations described so far, the EC of the parent vessel are initially in the immature state. The assumption is that the endothelium has reverted to a plastic phenotype in response to a tumour-derived signal, such as hypoxia. It is possible

that only a subset of the parent vessel is stimulated to enter the immature state, with the rest remaining in the mature state. We therefore ran a simulation in which the EC were initially in the immature state (p_1) for $x \in \left[\frac{1}{3}, \frac{2}{3}\right]$, and in the mature state (p_2) for $x \in \left[0, \frac{1}{3}\right) \cup \left(\frac{2}{3}, 1\right]$. The resulting time course for immature EC is shown in Figure 6.16 (as before, the EC behind the leading edge of the neovasculature mature to start to form stable vessels). Unsurprisingly, angiogenic growth is initially confined to the immature region. Nevertheless, as well as growing towards the tumour, the capillary tips spread outwards and the neovasculature, although always most advanced in $x \in \left[\frac{1}{3}, \frac{2}{3}\right]$, eventually grows to occupy all of $x \in [0, 1]$.

In this model, we have focussed on the expression of the angiopoietins by host cells: Ang-2 by immature EC and Ang-1 by peri-endothelial cells associated with mature vessels [99, 157]. It is possible that tumour cells also express angiopoietins [156], but expression patterns vary considerably between different tumour types and it is not always clear whether the secreted factors are derived from the tumour cells themselves, or from tumour-associated host cells [37, 144, 161]. Indeed, although it is known that hypoxia and various tumour-derived factors can upregulate Ang-2 expression, relatively little is known about the regulation of Ang-1 expression [70]. Furthermore, it has not yet been established whether expression of Ang-1 and/or Ang-2 by tumour cells has a positive or a negative effect on vascularisation of the tumour. In order to investigate this, we ran simulations (not shown) with a source of either Ang-1 or Ang-2 at the tumour (via a boundary condition of the form (6.26))[1]. The time until vascularisation was increased by Ang-1 expression by the tumour, and decreased by Ang-2 expression. The model thus predicts that tumour-derived Ang-1 will impede vascularisation, whereas tumour-derived Ang-2 will assist it.

As remarked in section 6.1.2, one could argue that the movement terms in (6.20) should be omitted, so that the mature EC are not capable of actively migrating. The results (not shown) of this are very similar to the full model (the time until vascularisation is slightly increased from 15.6 h to 16.3 h). It is an advantage of the model that it can predict stabilisation of the new vasculature without having to explicitly assume that the mature EC are inherently incapable of moving. Rather, the chemical microenvironment in the maturing part of the vessels is such that the

[1] Tumour-derived Ang-1/2 will not act as paracrine signalling factors as in the case of host cell-derived Ang-1/2, but must diffuse through the ECM in order to bind to the Tie-2 receptor on EC. Diffusive transport of the angiopoietins was therefore included in these simulations.

stimuli for migration (via the diffusivity (6.24) and transition probability function (6.25)) are much weaker than at the leading edge of the neovasculature.

6.5 Discussion

The model presented has, despite its relative simplicity, captured the key qualitative properties of the angiopoietins: Ang-1 as the stabilising factor and Ang-2 as the destabiliser. The main effects of Ang-1 and Ang-2 knockout and over-expression have been reproduced. Moreover, the model supports the emerging idea that Ang-2 is a critical regulator of angiogenic activity: an absence of Ang-2 allows Ang-1 to maintain vessels in the quiescent state; expression of Ang-2 allows either angiogenic outgrowth, or vessel regression, depending on the presence or absence of VEGF.

This may have implications for anti-angiogenic therapies that exploit the angiopoietins. For example, our results indicate that inhibition of Ang-2 or exogenous administration of Ang-1 may be able to impede angiogenesis. Such an approach is most likely to be successful in combination with another therapy, such as inhibition of VEGF or chemotherapy. Alternatively, if VEGF signalling can be effectively blocked, simultaneous administration of Ang-2 may lead to vessel regression. This strategy was identified in [95] as a potential anti-angiogenic therapy and our results support this idea. In particular, the results of delaying the onset of VEGF production by one hour suggest that such a strategy may be effective over a relatively short period of time. This may be relevant clinically because if, as is likely, the therapy does not eliminate the tumour colony but merely prevents further growth, then it will be necessary to give repeated and possibly indefinite applications. In such a scenario, a short treatment period is a major advantage.

The assumptions made, particularly the choice of functional forms (for example the motility coefficient (6.2) and proliferation function (6.6)) and parameter values, are open to question. The model is robust with respect to the unknown values (see section 6.3), but quantitative experimental data are required to determine these more precisely and to test model predictions. This would enable the assumptions to be critically reviewed and an improved model, capable of making quantitative, testable predictions, to be constructed.

We have focussed attention in this chapter on the angiopoietins because they have

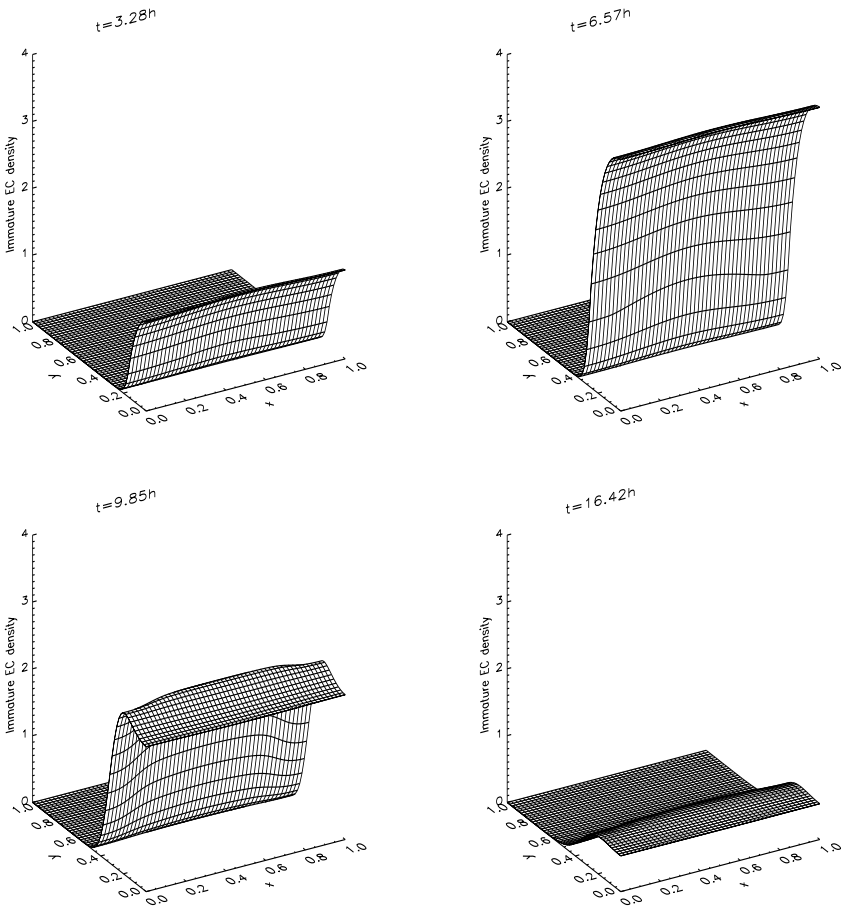

Figure 6.13: Time course for immature EC density with increased Ang-1 expression ($b_1 = 4560$ h^{-1}).

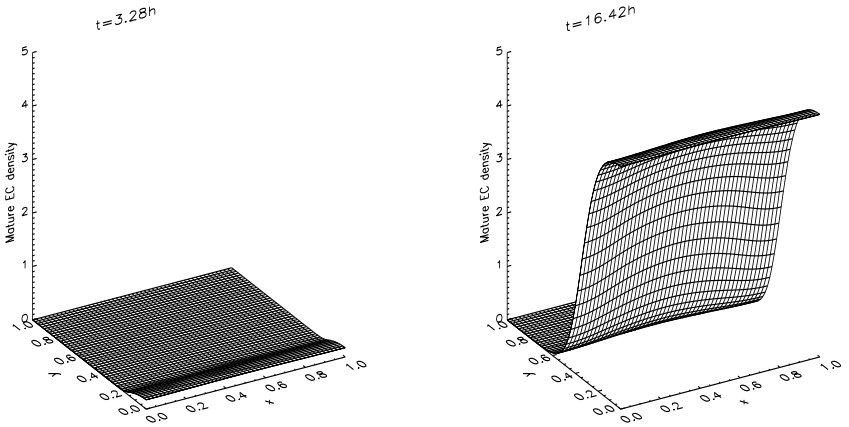

Figure 6.14: Time course for mature EC density with increased Ang-1 expression ($b_1 = 4560$ h^{-1}).

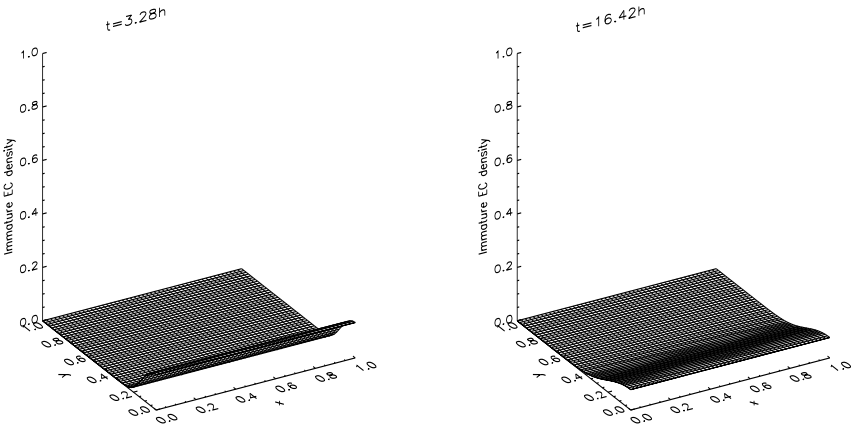

Figure 6.15: Time course for immature EC density with no VEGF ($v_0 = 0$).

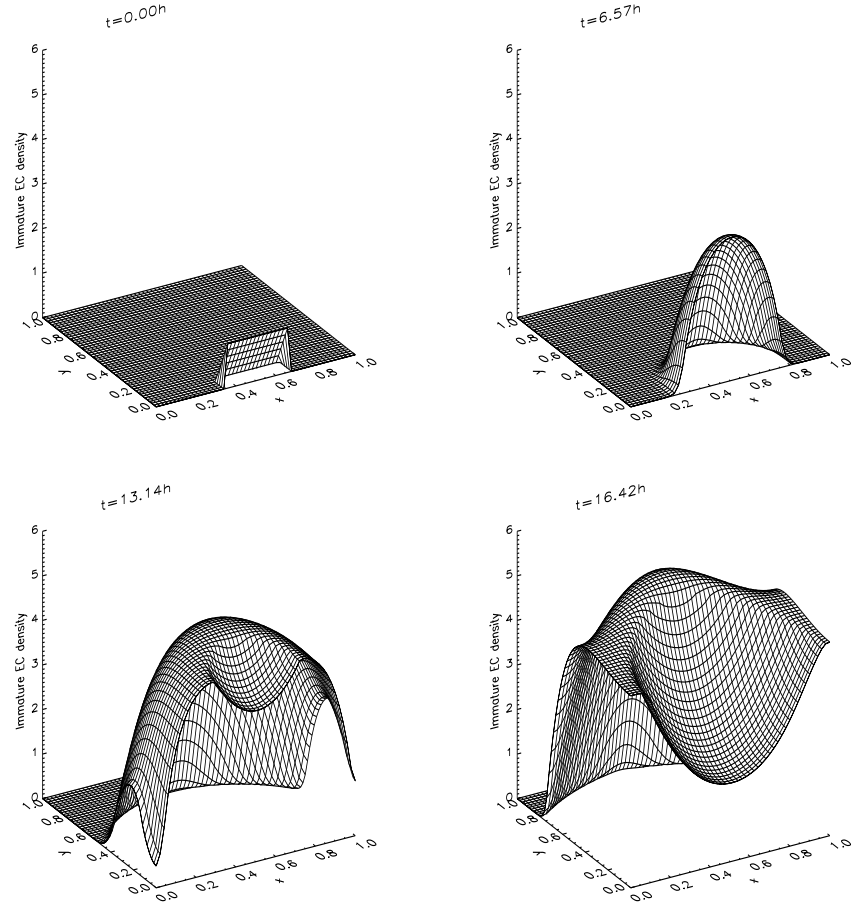

Figure 6.16: Time course for immature EC density with a modified initial condition: EC are initially in the immature state for $x \in \left[\frac{1}{3}, \frac{2}{3}\right]$ and in the mature state for $x \in \left[0, \frac{1}{3}\right) \cup \left(\frac{2}{3}, 1\right]$.

emerged as key regulators of angiogenesis, but have not yet been widely studied in a mathematical modelling context. Nevertheless, a complete model would also include other aspects of angiogenesis, such as haptotaxis and proteolysis of the ECM. Such considerations could be included in an extended model. A further important model extension would be to explicitly include a population of pericytes, which express Ang-1, instead of simply assuming that pericytes are automatically associated with the mature EC. This would enable the process of vessel maturation to be studied in a more realistic framework.

We have started with a continuum model of the angiopoietins in order to reproduce their main qualitative properties and to get a handle on the macroscopic behaviour. As has been discussed, such a model cannot capture the important microscopic features of angiogenesis, such as capillary branching and anastomosis. However, it is envisaged that a discrete form of the model will be constructed, enabling cell-based simulations to be carried out. Because the governing PDEs (6.19), (6.20) for EC density are in the form of the continuum limit of a reinforced random walk master equation, it should be mathematically straightforward to accomplish this.

6.6 Summary

- A continuous mathematical model for the role of the angiopoietins in tumour angiogenesis has been formulated and solved numerically.
- Model predictions are in qualitative agreement with experimental observations. In particular, inhibiting VEGF whilst administering Ang-2 is identified as a potential anti-angiogenic strategy.
- It would be straightforward to obtain a discrete form of the model, using the reinforced random walk master equation and transition probability function.
- Key references: Davis *et al.* [41], Maisonpierre *et al.* [99].